JOC Article

Theoretical Studies on Cycloaddition Reactions between 1-Aza-2-azoniaallene Cation and Olefins

Mei-Ju Wei, De-Cai Fang,* and Ruo-Zhuang Liu*

Department of Chemistry, Beijing Normal University, Beijing 100875, People's Republic of China

dcfang@bnu.edu.cn

Received April 29, 2002

Density functional (B3LYP) calculations using the 6-31++g** basis set have been employed to study the title reaction between the cationic 1,3-dipolar 1-aza-2-azoniaallene ion ($H_2C{=}N^+{=}NH$) and ethene. Our calculations confirmed that [3 + 2] cycloaddition reaction takes place via a three-membered ring intermediate. In addition, solvent effects and substituent effects were also studied. For the reactions involving tetrachloroethene, there are two attacking sites. One is on the NH group in the 1-aza-2-azoniaallene ion, another is on its terminal CH_2 group, and they are competitive for both approaching positions. Electron-releasing methyl substituents on ethene favor the reaction, and the potential energy surface is quite different from the previous one.

Introduction

1,3-Dipolar cycloaddition reactions of neutral 1,3-dipoles are widely used in the preparative organic chemistry.[1] High stereospecificity and stereoselectivity are the reason these reactions are synthetically so useful in the synthetic field.[2] Theoretical studies have also received extensive attention.[3] On the basis of a number of reports on stereochemical, kinetic, and theoretical studies, 1,3-dipolar cycloaddition reactions are believed to proceed through a concerted mechanism.[3a−l,4]

Recently, the cycloadditions of cationic four-electron-three-center components with multiple bonds aroused chemist's interest.[5] 1-Aza-2-azoniaallene salts, one of the novel cationic four-electron-three-center components, were found to undergo cycloadditions with multiple bonds via [3 + 2] cycloaddition reactions,[6] which open a new and potentially useful route for the construction of five-membered heterocycles. In many oxidative processes of hydrazones, 1-aza-2-azoniaallene cations are generated as reactive intermediates.[7] They can also be gained at low temperature from 1-chloroalkyl-azo compounds on treatment with Lewis acid such as $SbCl_5$ or $AlCl_3$,[6f] and the reaction of 1-aza-2-azoniaallene cations with electron-rich olefins could produce 4,5-dihydro-3*H*-pyrazolium salts under mild conditions.[6a−e] Most cycloadducts of 1-aza-2-azoniaallene salts with other multiple bonds undergo a [1,2]-shift spontaneously,[6d−i,8] but cycloadducts of 1-aza-2-azoniaallene salts with olefins are difficult to rearrange to 4,5-dihydro-1*H*-pyrazonlium salts.[6a−d] Experimentally the cycloadditions of 1-aza-2-azoniaallene cations to olefins have been already studied; however,

* To whom correspondence should be addressed. Fax: (+86) 10-62200567. Tel: (+86) 10-62208508.

(1) (a) Huisgen, R. *Angew Chem., Int. Ed. Engl.* **1963**, *2*, 265. (b) Huisgen, R. In *1,3-Dipolar Cycloaddition Chemistry*; Padwa, A., Ed.; Wiley: New York, 1984; Vol. 1, pp 1−176. (c) Cinquini, M.; Cozzi, F. In *Stereoselective Synthesis*; Helmchen, G., Hoffmann, R. W., Mulzer, J., Schauman, E., Eds.; Georg Thieme: Stuttgart, 1996; Vol. 5, pp 2953−2987. (d) Houk, K. N.; Yamaguchi, K. In *1,3-Dipolar Cycloaddition Chemistry*; Padwa, A., Ed.; Wiley: New York, 1984; Vol. 2, pp 407−450. (e) Padwa, A. In *Comprehensive Organic Synthesis*; Trost, B. M., Fleming, I., Eds.; Pergamon: Oxford, 1991; Vol. 4, pp 1069−1109. (f) Wade, P. A. In *Comprehensive Organic Synthesis*; Trost, B. M., Fleming, I., Eds.; Pergamon: Oxford, 1991; Vol. 4, pp 1111−1168.

(2) For examples, see: (a) Snider, B. B.; Lin, H. *J. Am. Chem. Soc.* **1999**, *121*, 7778. (b) Pandey, G.; Sahoo, A. K.; Gadre, S. R.; Bagul, T. D.; Phalgune, U. D. *J. Org. Chem.* **1999**, *64*, 4990. (c) Werner, K. M.; de los Santos, J. M.; Weinreb, S. M.; Shang, M. *J. Org. Chem.* **1999**, *64*, 4865. (d) Gong, Y. D.; Najdi, S.; Olmstead, M. M.; Kurth, M. J. *J. Org. Chem.* **1998**, *63*, 3081. (e) Lee, J. C.; Jin, S.-J.; Cha, J. K. *J. Org. Chem.* **1998**, *63*, 2804. (f) Tamura, O.; Mita, N.; Kusaka, N.; Suzuki, H.; Sakamoto, M. *Tetrahedron Lett.* **1997**, *38*, 429.

(3) For examples, see: (a) Poppinger, D. *Aust. J. Chem.* **1976**, *29*, 465. (b) Komornicki, A.; Goddard, J. D.; Schaefer, H. F., III. *J. Am. Chem. Soc.* **1980**, *102*, 1763. (c) McDouall, J. J. W.; Robb, M. A.; Niazi, U.; Bernardi, F.; Schlegel, H. B. *J. Am. Chem. Soc.* **1987**, *109*, 4642. (d) Esseffar, M.; Jalal, R.; Messaoudi, M. E.; Mouhtadi, M. E. *THEOCHEM* **1998**, *433*, 301. (e) Rastelli, A.; Gandolfi, R.; Amade, M. S. *J. Org. Chem.* **1998**, *63*, 7425. (f) Nguyen, M. T.; Chandra, A. K.; Sakai, S.; Morokuma, K. *J. Org. Chem.* **1999**, *64*, 65. (g) Valentin, C. D.; Freccero, M.; Gandolfi, R.; Rastelli, A. *J. Org. Chem.* **2000**, *65*, 6112. (h) Hu, Y.; Houk, K. N. *Tetrahedron* **2000**, *56*, 8239. (i) Rastelli, A.; Gandolfi, R.; Sarzi-Amade, M.; Carboni, B. *J. Org. Chem.* **2001**, *66*, 2449. (j) Blavins, J. J.; Karadakov, P. B. *J. Org. Chem.* **2001**, *66*, 4285. (k) Nguyen, L. T.; Proft, F. D.; Chandra, A. K.; Uchimaru, T.; Nguyen, M. T.; Geerlings, P. *J. Org. Chem.* **2001**, *66*, 6096. (l) Baranski, A. *THEOCHEM* **1998**, *432*, 229. (m) Caramella, P.; Houk, K. N.; Domelsmith, L. N. *J. Am. Chem. Soc.* **1977**, *99*, 4511. (n) Hiberty, P. C.; Ohanessian, G.; Schlegel, H. B. *J. Am. Chem. Soc.* **1983**, *105*, 719. (o) Dewar, M. J. S. *J. Am. Chem. Soc.* **1984**, *106*, 209. (p) Sosa, C.; Andzelm, J.; Lee, C.; Blake, J. G.; Chenard, B. C.; Butler, J. W. *Int. J. Quantum Chem.* **1994**, *49*, 511. (q) Williams, C. I.; Whitehead, M. A.; Jean-Claude, B. J. *THEOCHEM* **1999**, *491*, 103. (r) Vivanco, S.; Lecea, B.; Arrieta, A.; Prieto, P.; Morao, I.; Linden, A.; Cossio, F. P. *J. Am. Chem. Soc.* **2000**, *122*, 6078. (s) Tanaka, J.; Kanemasa, S. *Tetrahedron* **2001**, *57*, 899. (t) Baranski, A. *THEOCHEM* **2000**, *499*, 185.

(4) For examples, see: (a) Huisgen, R. *J. Org. Chem.* **1976**, *41*, 403. (b) Houk, K. N.; Firestone, R. A.; Munchausen, L. L.; Mueller, P. H.; Arison, B. H.; Garcia, L. A. *J. Am. Chem. Soc.* **1985**, *107*, 7227. (c) Avalos, M.; Babiano, R.; Cintas, P.; Clemente, F. R.; Gordillo, R.; Jiménez, J. L.; Palacios, J. C.; Raithby, P. R. *J. Org. Chem.* **2000**, *65*, 5089. (d) Houk, K. N.; Gonzalez, J.; Li, Y. *Acc. Chem. Res.* **1995**, *28*, 81.

(5) For examples, see: (a)Wirschun, W.; Jochims, J. C. *Synthesis* **1997**, 233. (b) Wirschun, W.; Winkler, M.; Lutz, K.; Jochims, J. C. *J. Chem. Soc., Perkin Trans. 1* **1998**, 1755. (c) Parsons, S.; Passmore, J.; Schriver, M. J.; Sun, X. *Inorg. Chem.* **1991**, *30*, 3342. (d) Burford, N.; Johnson, J. P.; Passmore, J.; Schriver, M. J.; White, P. S. *J. Chem. Soc., Chem. Commun.* **1986**, 966.

10.1021/jo0258709 CCC: $22.00
Published on Web 09/27/2002

CHART 1

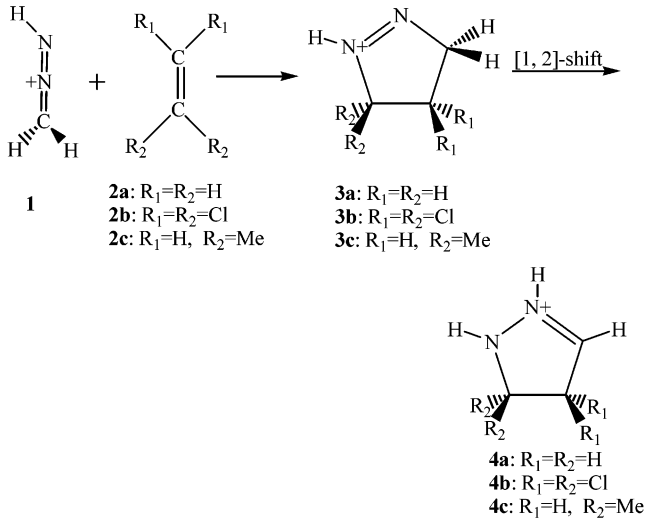

theoretical study, to our knowledge, still remains untouched. Therefore, we have employed a model reaction, $H_2C{=}N^+{=}NH + CH_2{=}CH_2$, as studied object to investigate the mechanism using density functional theory (DFT). Moreover, solvent effects and substitutent effects on the carbon in olefin are also investigated for comparison. The reactions considered are shown in Chart 1.

This work is one part of our research program devoted to the study of the cycloaddition of cumulenes.[9]

Methods of Calculation

Density functional calculations are carried out for [3 + 2] cycloaddition reactions between 1-aza-2-azoniaallene cations (**1**) and olefins. All calculations included in this work have been performed with the Gaussian 98w program package.[10] The geometries of reactants, products, complexes, intermediates, and transition states have been fully optimized. All geometric parameters of possible stationary points have been located at B3LYP/6-31++G** level and characterized by the number of imaginary frequencies. For some key reaction paths, intrinsic reaction coordinate (IRC)[11] has been traced to confirm the TS connecting with the corresponding two minima. The relative energies of all stationary points are corrected with 0.95 scaling factor of zero-point vibrational energies. For the model reaction, we employed the polarized continuum (overlapping spheres) model (PCM)[12] and solvent CH_2Cl_2 (dielectric constant $\epsilon = 8.93$) to calculate the solvent effects at 298.15 K.

Bader's theory of AIM[13] has been used to study the bonding character and charge distribution for some stationary points in our studied reactions. AIM98PC package,[14] a PC version of AIMPAC,[15] has been employed for the electron density topological analysis using the electron densities obtained by the B3LYP/6-31++G** calculation.

Results and Discussion

Model Reaction: $H_2C{=}N^+{=}NH + CH_2{=}CH_2$. The reaction is investigated in the gas phase at first, and two possible addition pathways in this reaction are discussed. The geometries of the reactants (**1** and **2a**), complexes (**COM1a** and **COM1b**), intermediates (**INT1a** and **INT1b**), transition states (**TS1a**, **TS1b**, **TS1c**, **TS1d**, **TS1e**, and **TS1f**), and products (**3a**, **4a,** and **5a**) are optimized at B3LYP/6-31++G** level, and all stationary points are characterized by vibrational frequencies. The atomic numbering systems of the above stationary points are shown in Figure S1 of Supporting Information and Scheme 1, and the optimized parameters, frequencies, and energies are listed in Tables S1−S3 of Supporting Information, respectively.

From the structural parameters it can be seen that one of the reactants, 1-aza-2-azoniaallene cation (**1**), is ap-

(6) For examples, see: (a) Wirschun, W. G.; Al-Soud, Y. A.; Nusser, K. A.; Orama, O.; Maier, G. M.; Jochims, J. C. *J. Chem. Soc., Perkin Trans. 1* **2000**, 4356. (b) Hassan, N. A.; Mohamed, T. K.; Abdel Hafez, O. M.; Lutz, M.; Karl, C. C.; Wirschun, W.; Al-Soud Y. A.; Jochims, J. C. *J. Prakt. Chem.* **1998**, *340*, 151. (c) Al-Soud, Y. A.; Wirschun, W.; Hassan, N. A.; Maier, G.-M.; Jochims, J. C. *Synthesis* **1998**, 721. (d) Wang, Q.; Amer, A.; Mohr, S.; Ertel, E.; Jochims, J. C. *Tetrahedron* **1993**, *49*, 9973. (e) Guo, Y.; Wang, Q.; Jochims, J. C. *Synthesis* **1996**, 274. (f) Wang, Q.; Jochims, J. C.; Kohlbrandt, S.; Dahlenburg, L.; Al-Taib, M.; Hamed, A.; Ismail, A. E. *Synthesis* **1992**, 710. (g) Wang, Q.; Amer, A.; Troll, C.; Fischer, H.; Jochims, J. C. *Chem. Ber.* **1993**, *126*, 2519. (h) Wang, Q.; Al-Taib, M.; Jochims, J. C. *Chem. Ber.* **1994**, *127*, 541. (i) Wang, Q.; Mohr, S.; Jochims, J. C. *Chem. Ber.* **1994**, *127*, 947. (j) Al-Masoudi, N.; Hassan, N. A.; Al-Soud, Y. A.; Schmidt, P.; Gaafar, A. E.-D. M.; Weng, M.; Marino, S.; Schoch, A.; Amer, A.; Jochims, J. C. *J. Chem. Soc., Perkin Trans. 1* **1998**, 947. (k) Al-Soud, Y. A.; Shrestha-Dawadi, P. B.; Winkler, M.; Wirschun, W.; Jochims, J. C. *J. Chem. Soc., Perkin Trans. 1* **1998**, 3759. (l) El-Gazzar, A. B. A.; Scholten, K.; Guo, Y.; Weiβenbach, K.; Hitzler, M. G.; Roth, G.; Fischer, H.; Jochims, J. C. *J. Chem. Soc., Perkin Trans. 1* **1999**, 1999. (m) Al-Masoudi, N. A.; Al-Soud, Y. A.; Geyer, A. *Tetrahedron* **1999**, *55*, 751. (n) Liu, X.; Zou, J.; Fan, Y.; Wang, Q. *Synthesis* **1999**, 1313. (o) Liu, X.; Liu, Y.; Wang, Q. *Synth. Commun.* **2000**, *30*, 119.

(7) (a) Okimoto, M.; Chiba, T. *J. Org. Chem.* **1990**, *55*, 1070. (b) Lin, E.-C.; Van De Mark, M. R. *J. Chem. Soc., Chem. Commun.* **1982**, 1176. (c) Hammerich, O.; Parker, V. D. *J. Chem. Soc., Perkin Trans. 1* **1972**, 1718. (d) Crljenak, S.; Tabakovic, I.; Jeremic, D.; Gaon, I. *Acta Chem. Scand.* **1983**, *B37*, 527. (e) Gunic, E.; Tabakovic, I. *J. Org. Chem.* **1988**, *53*, 5081. (f) Butler, R. N. *Chem. Rev.* **1984**, *84*, 249. (g) Warkentin, J. *Synthesis* **1970**, 279.

(8) For examples, see: (a) Gstach, H.; Seil, P. *Synthesis* **1990**, 803. (b) Gstach, H.; Seil, P. *Synthesis* **1990**, 808. (c) Gstach, H.; Seil, P. *Synthesis* **1990**, 1048. (d) Kroemer, R. T.; Gstach, H.; Liedl, K. R.; Rode, B. M. *J. Am. Chem. Soc.* **1994**, *116*, 6277. (e) Kroemer, R. T.; Gstach, H.; Liedl, K. R.; Rode, B. M. *J. Chem. Soc., Perkin Trans. 2* **1994**, 2129.

(9) (a) Fang, D. C.; Fu, X. Y. *Chem. Phys. Lett.* **1996**, *259*, 265. (b) Fang, D. C.; Fu, X. Y. *Chinese J. Chem.* **1996**, *14*, 97. (c) Fang, D. C.; Xu, Z. F.; Fu, X. Y. *THEOCHEM* **1995**, *333*, 159. (d) Fang, D. C.; Fu, X. Y. *J. Quantum Chem.* **1996**, *57*, 1107. (e) Sheng, Y. H.; Fang, D. C.; Wu, Y. D.; Fu, X. Y.; Jiang, Y. S. *THEOCHEM* **1999**, *488*, 187. (f) Ding, W. J.; Fang, D. C. *J. Org. Chem.* **2001**, *66*, 6673. (g) Yang, S. Y.; Sun, C. K,; Fang, D. C. *J. Org. Chem.* **2002**, *67*, 3841.

(10) Frisch, M. J.; Trucks, G. W.; Schlegel, H. B.; Scuseria, G. E.; Robb, M. A.; Cheeseman, J. R.; Zakrzewski, V. G.; Montgomery, J. A., Jr.; Stratmann, R. E.; Burant, J. C.; Dapprich, S.; Millam, J. M.; Daniels, A. D.; Kudin, K. N.; Strain, M. C.; Farkas, O.; Tomasi, J.; Barone, V.; Cossi, M.; Cammi, R.; Mennucci, B.; Pomelli, C.; Adamo, C.; Clifford, S.; Ochterski, J.; Petersson, G. A.; Ayala, J. B.; P. Y.; Cui, Q.; Morokuma, K.; Malick, D. K.; Rabuck, A. D.; Raghavachari, K.; Foresman, J. B.; Cioslowski, J.; Ortiz, J. V.; Baboul, A. G.; Stefanov, B. B.; Liu, G.; Liashenko, A.; Piskorz, P.; Komaromi, I.; Gomperts, R.; Martin, R. L.; Fox, D. J.; Keith, T.; Al-Laham, M. A.; Peng, C. Y.; Nanayakkara, A.; Challacombe, M.; Gill, P. M. W.; Johnson, B.; Chen, W.; Wong, M. W.; Andres, J. L.; Gonzalez, C.; Head-Gordon, M.; Replogle, E. S.; Pople, J. A. *Gaussian 98*, revision A.9; Gaussian, Inc.: Pittsburgh, PA, 1998.

(11) (a) Gonzalez, C.; Schlegel, H. B. *J. Chem. Phys.* **1989**, *90*, 2154. (b) Gonzalez, C.; Schlegel, H. B. *J. Phys. Chem.* **1990**, *94*, 5523.

(12) (a) Miertus, S.; Scrocco, E.; Tomasi, J. *J. Chem. Phys.* **1981**, *55*, 117. (b) Miertus, S.; Tomasi, J. *J. Chem. Phys.* **1982**, *65*, 239. (c) Cossi, M.; Barone, V.; Cammi, R.; Tomasi, J. *J. Chem. Phys. Lett.* **1996**, *255*, 32. (d) Cances, M. T.; Mennucci, V.; Tomasi, J. *J. Chem. Phys.* **1997**, *107*, 3032. (e) Barone, V.; Cossi, M.; Mennucci, B.; Tomasi, J. *J. Chem. Phys.* **1997**, *107*, 3210. (f) Cossi, M.; Barone, V.; Mennucci, B.; Tomasi, J. *Chem. Phys. Lett.* **1998**, *286*, 253. (g) Barone, V.; Cossi, M.; Tomasi, J. *J. Comput. Chem.* **1998**, *19*, 404. (h) Barone, V.; Cossi, M. *J. Phys. Chem. A* **1998**, *102*, 1995. (i) Mennucci, B.; Tomasi, J. *J. Chem. Phys.* **1998**, *109*, 249.

(13) (a) Bader, R. F. W. *Chem. Rev.* **1991**, *91*, 983. (b) Bader, R. F. W. *Atoms in Molecules, a Quantum Theory*; Clarendon Press: Oxford, 1990.

(14) Fang, D.-C.; Tang, T.-H. *AIM98PC*, the PC version of AIMPAC; Beijing Normal University: Beijing, China, 1998.

(15) Available from Professor R. F. W. Bader's Laboratory, McMaster University, Hamilton, Ontario, Canada L8S 4M1.

SCHEME 1

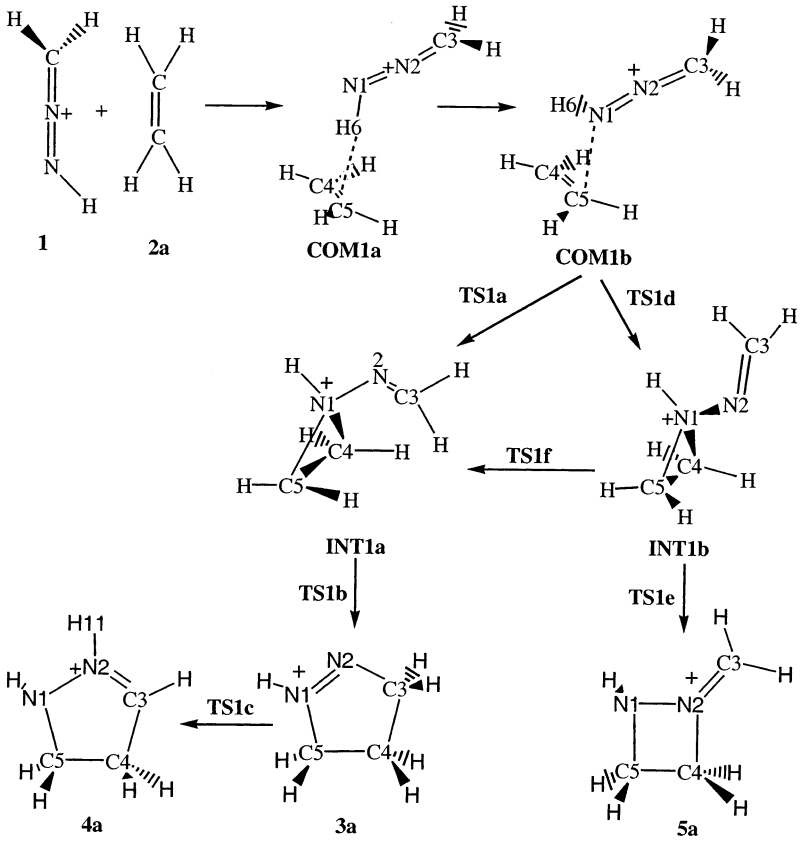

proximately a linear molecule with the angle C−N−N being 170.7°. The hydrogen atom connected to the nitrogen is almost on the same plane with its skeleton atoms (H−N−N−C = −179.9°), while the plane of methylene is perpendicular to the C−N−N plane (H−C−N−N = 90.9°).

Because the interaction between reactants yields ion−molecule complexes first, two complexes, denoted as **COM1a** and **COM1b** in Scheme 1, have been located. **COM1a** is a typical π-type hydrogen-bonded complex, in which the distances C5−H6 and C4−H6 are 2.091 and 2.091 Å, respectively. The C5−C4−C3−N2 dihedral angle of −76.8° in **COM1a** shows that the two reactants approach in gauche mode. When the two reactants further approach, **COM1b** is formed, which is a typical molecular complex (C5−N1 = 2.746 Å, C4−N1 = 3.002 Å).

For the pathway to form **3a** and **4a**, an intermediate **INT1a** is formed via **TS1a** first, and then the five-membered heterocycle **3a** is gained via **TS1b**, the last step from **3a** to **4a** is a hydrogen transfer process. Although the earlier computational studies on cycloaddition reactions involving unsubtituted 1,3-dipoles and dipolarophiles indicated that these reactions usually follow concerted pathways to produce five-membered heterocycles, our computation on the reaction **1** + **2a** to produce **3a** proves to be a stepwise mechanism with an intermediate **INT1a**. It can be realized from the optimized geometric parameters that when N1 approaches carbon atoms of ethene, the C3 atom of **1a** bends to the side of ethene (C3−N2−N1 = 169.4°, 140.7°, and 117.4° in **COM1b**, **TS1a**, and **INT1a**, respectively). Bond lengths of N1−N2 are 1.198, 1.263, and 1.443 Å for **COM1b**, **TS1a**, and **INT1a**, respectively, with a similar trend for C5−C4 bond lengths (1.346, 1.381, and 1.478 Å respectively). New bonds of N1−C5 and N1−C4 are formed in **INT1a** (1.506 Å), which is a cationic three-membered ring with the positive charges mainly in the ring (the charge of CH_2 groups in the ethene portion is 0.26 e and that of NH group is 0.18 e). Usually, the three-membered ring **INT1a** is not so stable that could take place the ring enlargement to the five-membered one via **TS1b**. This process is characterized by the change of the dihedral angle C5−C4−C3−N2 from −81.6° in **INT1a** to −59.6° in **TS1b** and then to 7.2° in **3a**. It can also be seen from the geometric parameters that the bond C3−C4 is mainly formed after **TS1b** (3.021, 2.904, and 1.549 Å for **INT1a**, **TS1b**, and **3a**, respectively), and the five-membered ring product is formed with the transfer of double bond from N2−C3 to N2−N1. The atoms in the ring of **3a** are almost at the same plane (C5−C4−C3−N2 = 7.2°, C4−C3−N2−N1 = −4.5°, H6−N1−N2−C3 = −179.1°), and the N1−N2 bond in **3a** is of double bond character with positive charge mainly settled on N1.

In most cases, rearrangements of cycloadducts between 1-aza-2-azoniaallene salts and multiple bonds could take place spontaneously via [1,2]-shift with the atom or group connected to the methylene migrating to the adjacent nitrogen atom;[6d−i,8] therefore, the rearrangement product 4,5-dihydro-1*H*-pyrazolium ion **4a** was also studied. The ring in **4a** is somewhat distorted (C5−C4−C3−N2 = 12.2°, C4−C3−N2−N1 = 2.7°). As a result of the migration of H11 from C3 to N2, the positive charge is transferred from N1 to N2; at the same time, the N2−C3 bond (1.290 Å) is of double bond character while N2−

N1 bond (1.389 Å) becomes a single bond in **4a**. **TS1c** is a transition state for [1,2]-shift from **3a** to **4a**, in which the distances of H11−C3 and H11−N2 are 1.432 and 1.227 Å, respectively, and the dihedral angle H11−C3−N2−N1 is 112.9°.

Another possible pathway is to form a four-membered ring product **5a**. **INT1b** is similar to **INT1a** but with the CH_2 group in the **1** portion bending out of the ethene fragment (the angle C3−N2−N1 is 114.7°). It is also a three-membered ring structure with the N1−C5 and N1−C4 bond lengths being 1.504 Å and the dihedral angle C5−C4−C3−N2 being 65.0°. We failed to locate a transition state connecting with **INT1b** and **3a**, but a transition state **TS1f** was located for the transformation between **INT1b** and **INT1a**, in which the angle C3−N2−N1 is 179.3°. Because most reactions of cumulenes with olefins will produce four-membered ring products,[9e,f] the similar product **5a** in this model reaction has been investigated for comparison. The skeleton atoms in **5a** are slightly distorted from the plane (C5−C4−C3−N2 = −8.3°, C4−C3−N2−N1 = −178.4°, H11−C3−N2−N1 = −176.9°). Because the three-membered ring intermediate **INT1b** is unstable, it can be opened with N1−C4 bond being broken and thus form a more stable four-membered ring product **5a**. In **TS1e**, the framework atoms are in gauche mode (C5−C4−C3−N2 = 39.3°) and the distance between N2 and C4 is still quite long (2.527 Å). The possible reaction path for this reaction is summarized in Scheme 1.

The schematic potential energy surface for the model reaction (with 0.95 scaling factor of zero-point energy correction) is given in Figure 1. Figure 1 reveals that **COM1a** is more stable than reactants by 11.8 kcal/mol as a result of the existence of the hydrogen bond and plus charge and **COM1b** is less stable than **COM1a** by 4.7 kcal/mol. The formation of **INT1a** needs to overcome only 5.7 kcal/mol activation barrier from **COM1b**, but that of **INT1b** needs to cover a higher activation barrier of 15.9 kcal/mol from **COM1b**. So **INT1a** is more easily formed. If **INT1b** is produced, it is difficult for it to turn into **5a** or **INT1a** with the comparatively high activation barrier being 32.3 or 41.1kcal/mol. Therefore, the favorable pathway is **1** + **2a** → **COM1a** → **COM1b** → **INT1a** → **3a** → **4a** under high-pressure gas phase. **INT1a** must get over the activation barrier of 38.6 kcal/mol to form a more stable product **3a**, which might take part in a [1,2] H-shift reaction to produce **4a** with an activation barrier of 38.5 kcal/mol. Our calculations, in fact, rationalize the experimental fact that no four-membered ring product could be found in such reactions.[6a−e] IRC calculations starting from **TS1a**, **TS1b**, and **TS1d** have been performed to confirm that these transition states could reach the minima at both sides of them shown in Figure 1.

The earlier works on cycloadditions involving unsubstituted 1,3-dipoles and dipolarophiles indicate that these reactions follow concerted pathways to produce five-memebered heterocycles, but the mechanism for the present reaction is quite different. Such difference can be explained with the frontier orbital interaction. Because the energy between the LUMO of **1** and HOMO of **2a** is much smaller than that between the LUMO of **2a** and HOMO of **1**, the former interaction is in the highest flight (shown in Figure 2a), which first results in three-membered ring intermediate **INT1a**. This can also be seen from the Laplacian distributions of electron density

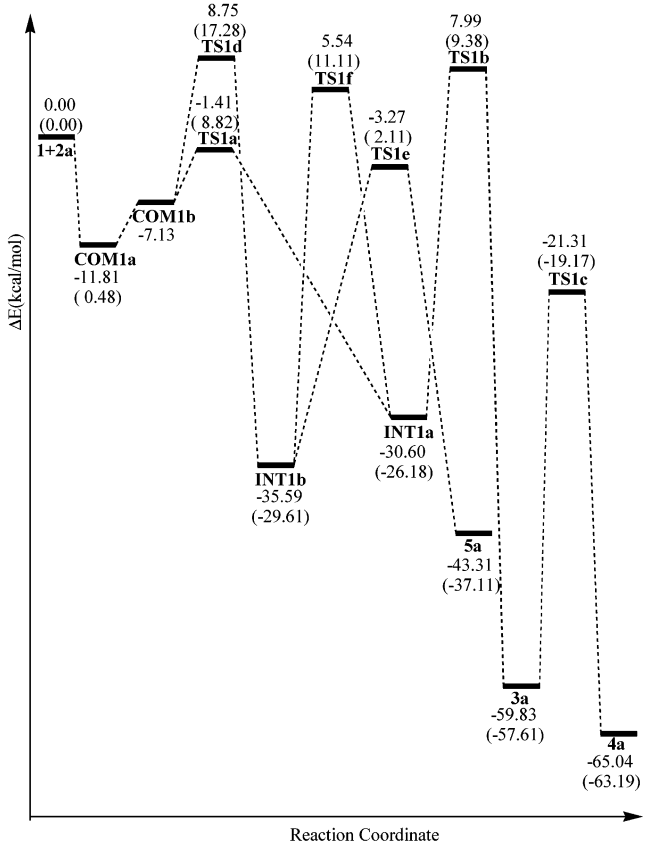

FIGURE 1. The schematic potential energy surface for the mechanism of the reaction **1** + **2a** (data in parentheses are for solution phase).

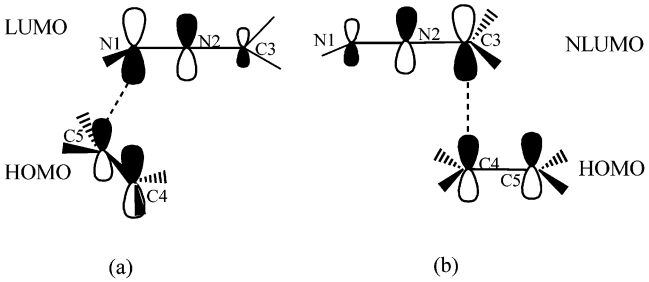

FIGURE 2. (a) The interaction between the LUMO of **1** and the HOMO of **2a**. (b) The interaction between the NLUMO of **1** and the HOMO of **2b**.

shown in Figure 3, from which one can realize that **COM1a** is a typical hydrogen-bonded complex and only one loose bond (C5−N1) exists in **COM1b** and **TS1a**.

The solvent effect of the model reaction has also been investigated. It is found that the structures of all stationary points (see Table S1 of Supporting Information) are in excellent agreement with those in gas phase. From the data in parentheses of Figure 1 and Table S3, one can see that cumulene **1** in solution phase is much more stable than that in gas phase, which is in good accordance with the fact that cumulene **1** is decomposed during evaporation of the solvent as described by Wang et al.[6f] **COM1a**-like complex in solution phase is only 0.8 kcal/mol lower than reactants without zero-point energy correction. If considered with 0.95 zero-point energy, **COM1a** in solution phase is above the reactants by 0.5

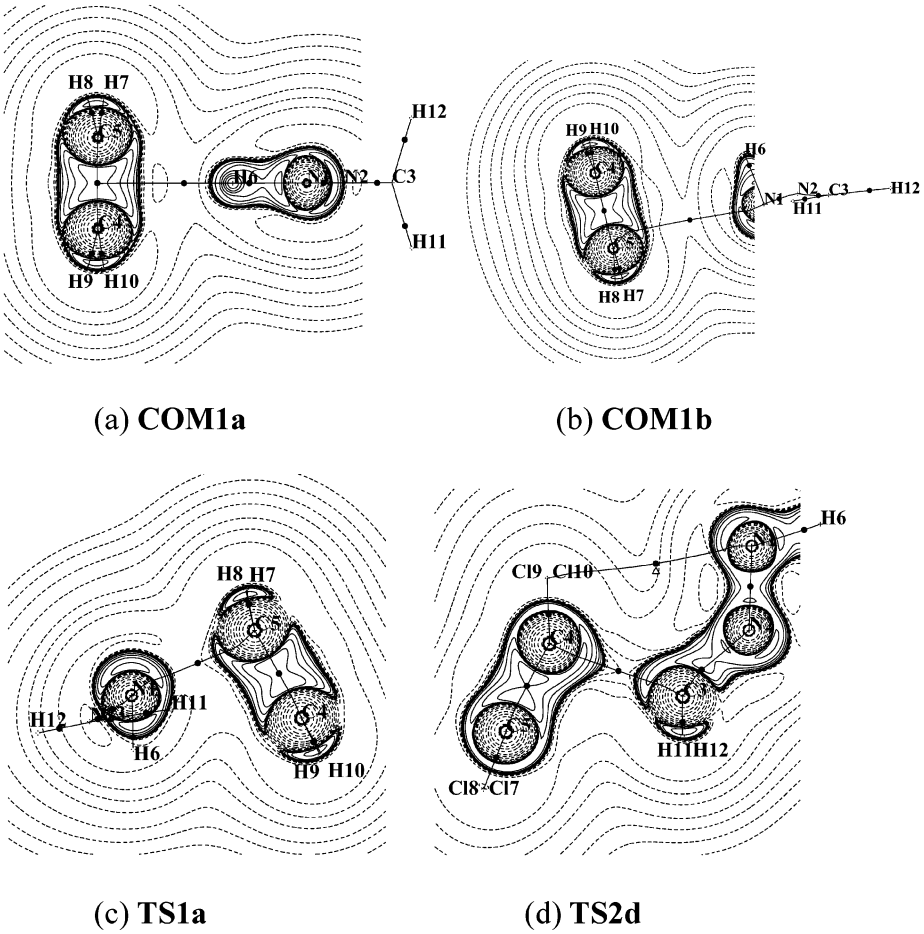

FIGURE 3. The molecular graphs and Laplacian distribution of some stationary points. In these figures, dashed lines denote positive values of $\nabla^2\rho_b$ and full lines stand for negative values of $\nabla^2\rho_b$. The bonded charge concentrations are indicated by solid squares. In addition, bond paths (heavy solid lines), bond critical points (solid circle), and ring critical points (triangle) are shown for ρ(r).

kcal/mol, which means that such hydrogen-bonded complex might not exist in solution phase because of solvent effect. The less stable complex **COM1b** could not been found in solution phase. The reaction passes through **TS1a** to form **INT1a** directly with an activation barrier of 8.8 kcal/mol from reactants, which is 3.1 kcal/mol higher than that from **COM1b** to **INT1a** in gas phase. For the rate-determinating step leading to **3a**, the activation barrier is 3.0 kcal/mol lower than that in gas phase.

Substituent Effect on Carbon in Ethene with Electron-Withdrawing Groups. In this section, we tried to investigate the substituent effect on the carbon atom in ethene with electron-withdrawing Cl groups (see Scheme 2). Since four-membered product is not preferential as discussed in the previous section and experimental results, we only discuss the possible pathways to form five-membered ring products afterward. The numbering systems and relative energies of the stationary points for reaction **1** + **2b** are given in Scheme 2 (also in Figure S2) and Figure 4, and the optimized geometric parameters, frequencies, and energies are listed in Tables S4−S6, respectively. As shown in Scheme 2, both a hydrogen-bonded complex **COM2** and three-membered ring intermediate **INT2a** could be located. **COM2** has stabilization energy of 5.6 kcal/mol. The dihedral angle of C5−C4−C3−N2 in **COM2** is changed to be −152.4° from −76.8° in the model reaction, so as to release steric hindrance arising from four chlorine atoms. At the same time, the distances of H6−C5 and H6−C4 become 2.114 and 2.322 Å, respectively. The N1−C5 and N1−C4 bonds in **INT2a** are longer by 0.064 Å than those in **INT1a** in model reaction because of four chlorine atoms, which leads to **INT2a** not being as stable as **INT1a** in the model reaction. The calculated activation barrier for the step from **INT2a** to **3b** is only 8.9 kcal/mol, which is 29.7 kcal/mol less than the rate-controlling step from **INT1** to **3a** in the model reaction. In reaction **1** + **2b**, the rate-determinating step becomes the first step with the activation barrier being 12.6 kcal/mol (see Figure 4), indicating that reaction **1** + **2b** can take place more easily than the model reaction as a result of the steric effect and super-conjugation of chlorine atoms. As far as relative energies are concerned, **3b**, the compound with four substituents, is not so stable as **3a** without any substituent. Despite the existence of substituent groups, it is still difficult for **3b** to rearrange to **4b** via **TS2c** with the activation barrier being 36.1 kcal/mol, which is only 2.4 kcal/mol lower than that in the model reaction. In fact, no [1,2] H-transfer rearrangement could be found in experiments.

SCHEME 2

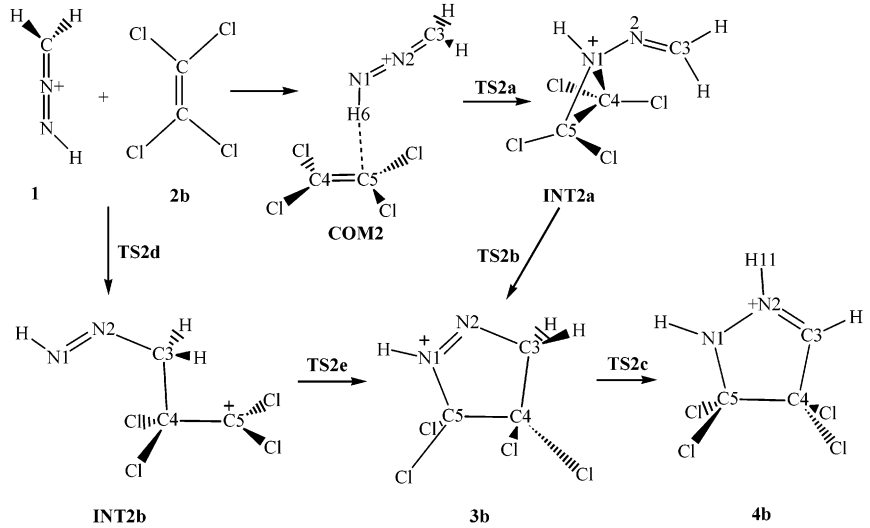

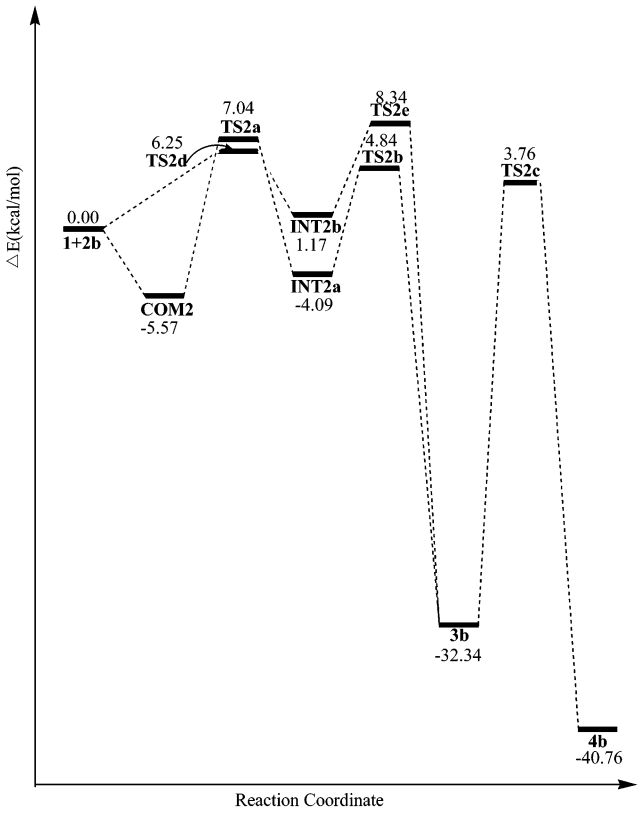

FIGURE 4. The schematic potential energy surface for the mechanism of reaction **1** + **2b**.

Interestingly, we found another reaction pathway leading to **3b**. It is also a two-step process, which contains one intermediate (**INT2b**) and two transition states (**TS2d** and **TS2e**), whose numbering systems are shown in Scheme 2 and Figure S2. The carbon atom in ethene attacking the terminal carbon atom C3 in **1** leads to an intermediate **INT2b**, which is a typical carbonium (the cation mainly holds on terminal $C(Cl)_2$ group in ethene). The distance of C4−C3 in **INT2b** is 1.601 Å, slightly longer than that of a normal C−C bond. The transition state (**TS2d)** for the formation of **INT2b** is of a trans structure with the distances of C4−C3 and C5−N1 being 2.068 and 4.437 Å, respectively. **TS2e** connects **INT2b** with **3b**, in which the dihedral angle C5−C4−C3−N2 is −123.5°. As the dihedral angle C5−C4−C3−N2 decreases, the distance between C5 and N1 decreases and thus **3b** is produced without a gauche intermediate. The formation of **INT2b** can also be rationalized by the frontier orbital interaction in Figure 2b and Laplacian distribution of electron density in Figure 3d. Because the energy level of the antibonding orbital of N═N (LUMO) in **1** is very close to that of C═N (NLUMO), the main orbital interaction for the latter pathway is that between HOMO of ethene and NLUMO of **1**, which leads to a stable carbonium. Figure 4 shows relative energies for the possible stationary points along these two pathways, which indicates that the two pathways are competitive. Our calculations confirm that the activation barriers to form **3b** is quite low, which is in a good agreement with experimental fact that Cl-substituted ethene could easily react with 1-aza-2-azoniaallene cation.[6a]

Substituent Effect on Carbon in Ethene with Electron-Releasing Groups. In this section, two methyl groups are introduced into the same carbon atom C5 in ethene (denoted as **1** + **2c**). Two possible ortho and para products could be located, but only the preferential ortho product is considered here for convenience. Scheme 3 shows the two possible pathways in the reaction of **1** + **2c**, and the schematic potential energy surface is given in Figure 5, which shows that all stationary points are well below the reactant asymptote. In this reaction, the potential energy surfaces are quite different from the previous ones. Two stable intermediates (**INT3a** and **INT3b**) have been located with the stabilization energy of more than 30 kcal/mol and are similar in geometric parameters with **INT2a** and **INT2b**. Extensive searches for the possible transition states between **1** + **2c** and **INT3a** or **INT3b** always reach **1** + **2c**, i.e., no transition states between them could be found. The numbering system of all stationary points are given in Scheme 3 and Figure S3, and the optimized parameters, frequencies, and energies for this reaction are listed in Tables S7−S9 of Supporting Information, respectively.

In the first pathway, the carbon atoms in ethene approach the terminal nitrogen atom in **2c** to form three-

SCHEME 3

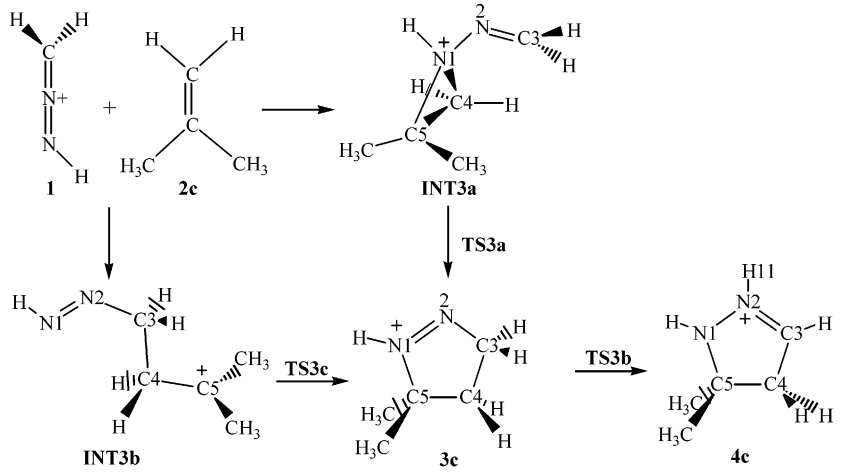

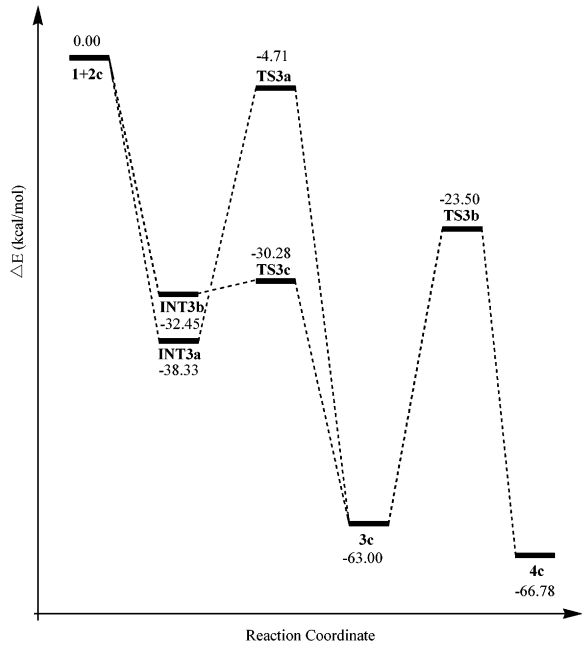

FIGURE 5. The schematic potential energy surface for the mechanism of **1** + **2c**.

membered ring cation **INT3a** with N1−C4 and N1−C5 being 1.502 and 1.528 Å, respectively. Since the methyl groups are the electron-releasing ones, the CH_3 groups make the ethene richer in electrons and thus more easily form the intermediate with electron-deficient **1**. The three-membered ring cation **INT3a** is more stable than **INT1a** in the model reaction and the ring in **INT3a** seems easier to be opened, with the activation barrier 5.0 kcal/mol lower than that in the model reaction. In addition, [1,2] H-shift from **3c** to **4c** via **TS3b** is also with high activation barrier of 39.5 kcal/mol.

In the second pathway, the carbon atom without CH_3 groups in ethene collides with carbon atom in **1** to form **INT3b** directly without climbing up a transition state like **TS2d** in reaction **1** + **2b**. **INT3b** is a steady cation with positive charge mainly located in C5 owing to the two CH_3 groups connected with C5. The energy of **INT3b** is 32.5 kcal/mol lower than that of reactants, while **INT2b** in reaction **1** + **2b** is 1.2 kcal/mol higher than that of reactants. The energy of **TS3c** is 30.3 kcal/mol lower than that of reactants, whereas the energy of **TS2e** is 8.3 kcal/mol below reactants. The formation of **3c** from **INT3b** needs to cover only 2.2 kcal/mol activation barrier, much lower than the process from **INT3a** to **3c** via **TS3a** (33.6 kcal/mol); therefore, the reaction occurs mainly through the pathway containing a trans carbonium **INT3b** and a transition state **TS3c**. In experiments, such reactions could occur at very low temperatures (about 193 K), which is in a good agreement with our calculated results in Figure 5.

Taking account of frontier orbital interaction, the electron-pushing substituted groups increase the energy level of HOMO in olefin, which in turn leads to a lower energy difference between the HOMO of **2a** and the NLUMO or LUMO of **1** and favors the formation of intermediates **INT3a** and **INT3b**. Moreover, the introduction of CH_3 groups will also disperse the positive charge on N1 and stabilize the **INT3b**.

Summary

The reaction **1** + **2a** in gas phase, namely, the model reaction, takes place via two transition states, one complex, and one intermediate. In CH_2Cl_2 solution, the basic reaction scheme is similar to that in gas phase, but the hydrogen-bonded complex becomes less stable.

Substituents on the carbon atoms in olefin have a notable effect on the mechanism and reaction barrier. Reactions with Cl groups in olefin are competitive for both attacking sites, while the electron-releasing methyl substituent groups in olefin favor the reaction with attacking CH_2 group in **1**. The energy surface of the latter is distinct from the former. All the stationary points are well below the reactant asymptote, in which two stable intermediates are formed from **1** + **2c** without activation barriers.

Acknowledgment. This work was supported by National Natural Science Foundation of China (No. 20073006) and authors also thank Prof. Ting-Hua Tang for language polishing.

Supporting Information Available: The Z-matrixes, frequencies and energies of all the stationary points are listed in Table S1−S9. This material is available free of charge via the Internet at http://pubs.acs.org.

JO0258709